Journal of Chromatography, 515 (1990) 193–204
Elsevier Science Publishers B.V., Amsterdam

CHROMSYMP. 1899

Binding capacities of hydroxyapatite for globular proteins

SENYA INOUE* and NOBUYUKI OHTAKI
Central Research Laboratory, Kanto Chemical Co., Inc., 1-7-1, Inari Soka-City, Saitama 340 (Japan)

ABSTRACT

The binding capacities of hydroxyapatite (HAP) for globular proteins depended on the effective surface area for adsorption, described as $(S_{BET} - S_p)px$, where S_{BET} is the BET surface area, S_p is the accumulation of surface areas based on small pores which the tested protein cannot enter, p is the proportion of the area of the adsorbing surface connected with basic or acidic proteins and x is the proportion of the area of the active part of each type of adsorbing surface. The values of px and $(S_{BET} - S_p)$ varied with the preparation methods and condition of HAP.

INTRODUCTION

The hydroxyapatite (HAP) crystal has two types of main adsorbing surfaces which are related to the binding of basic and acidic proteins[1,2]. The proportion of the area of each type of adsorbing surface, the state of the adsorbing surface and the BET surface area are considered to be affected by the preparation methods and condition of HAP. For example, HAP crystallized in aqueous solution tends to grow along the c axis and the surfaces parallel to the $\{10\bar{1}0\}$ planes develop mostly on the crystal surface[3–5]. On the other hand, spherical and sintered polycrystalline HAPs have been developed during the last few years with improvements in their mechanical strength for use as packing materials[6–9]. Based on their preparation methods it is considered that they have almost equal proportions of the areas of each type of adsorbing surface. Further, polycrystalline HAP surfaces have lattice defects due to the presence of grain boundaries and some deficiencies of lattice hydroxyl groups, which affect the completeness of the surface state[10]. These differences in surface state are suggested to affect the binding capacities for proteins. Hence the binding capacities of HAP cannot be interpreted solely from the dependence on surface areas measured by the BET method.

In this work we studied the effect of the surface states of HAP on the binding capacities for globular proteins. Spherical HAPs with different surface states were prepared by the spray method and heat treatments at various temperatures in air. For comparison of the effects of preparation methods on surface states, commercially available HAPs prepared by wet processes were also tested. Surface states were

0021-9673/90/$03.50

determined by X-ray diffraction analysis, differential thermal and thermogravimetric analysis, infrared spectrophotometry and scanning electron microscopy (SEM).

EXPERIMENTAL

HAP packing materials

Spherical HAP packing materials (HAP-1–5) were prepared as follows. HAP crystals with diameters of the order of 0.1 μm as starting material were precipitated by mixing a $Ca(NO_3)_2$–CH_3OH–H_2O solution and an H_3PO_4–CH_3OH–H_2O solution. The HAP slurry thus obtained was then spray-pyrolysed. The droplets when sprayed into a flame were instantaneously dried and sintered into spherical and porous polycrystals by heat of combustion of the vaporized CH_3OH. These spherical and sintered HAP packing materials were heat treated at 700–1000°C for 4 h in air to change the physical and chemical properties of the HAP surface. HAP-6 and -7 were prepared by wet processes. Table I summarizes the properties of the HAP samples tested. Fig. 1 illustrates the scanning electron microscopy (SEM) photographs of the surfaces of these HAPs.

Proteins

The proteins used are listed in Table II. Bovine serum albumin (BSA) and lysozyme were obtained from Merck (Darmstadt, F.R.G.) and all other proteins from Sigma (St. Louis, MO, U.S.A.). They were all globular proteins with a frictional ratio range of 1.1–1.3.

Binding capacities

Seven samples of HAP with different surface states were packed in 100 mm × 8 mm ID. stainless-steel columns. The maximum amount of proteins loaded

TABLE I

PROPERTIES OF HYDROXYAPATITES USED

For details of preparations and measurements, see Experimental.

Sample	*Preparation*	*Phase*	*BET surface area (m^2/g)*	*Weight loss[a] (%)*	*Intensity of OH^- frequency[b]*	
					New sample	*Sample used for HPLC*
HAP-1	Spray method	HAP	21.8	0	100	100 × 1.04[c]
HAP-2	Heating of HAP-1 at 700°C	HAP	18.0	0.8	96	96 × 1.04
HAP-3	Heating of HAP-1 at 800°C	HAP	14.4	1.3	84	84 × 1.09
HAP-4	Heating of HAP-1 at 900°C	HAP	6.4	1.4	72	72 × 1.12
HAP-5	Heating of HAP-1 at 1000°C	HAP+α-TCP	1.9	1.7	45	45 × 1.31
HAP-6	Wet process	HAP	7.8	–	–	–
HAP-7	Wet process	HAP	32.4	–	–	–

[a] Calculated by $[(W_0 - W)/W_0] \cdot 100$, where W_0 and W are weight of HAP-1 before and after heating at a given temperature.

[b] Intensity (arbitrary units) of the hydroxyl stretching frequency at 3572 cm^{-1}.

[c] The intensity of the OH^- frequency (= 104 in arbitrary units) of the sample used for HPLC increased by 4% compared to that (= 100) of the new sample. This is similar for the other HAP samples.

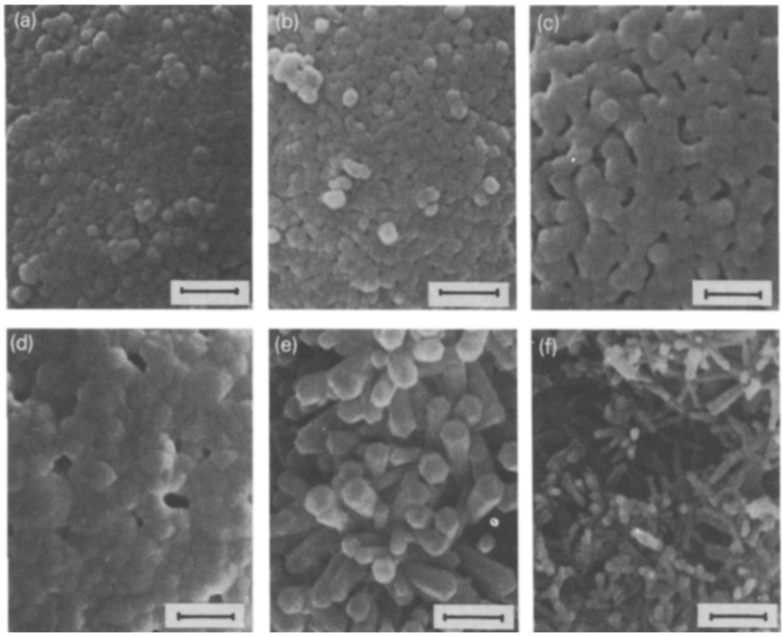

Fig. 1. SEM photographs of hydroxyapatite packing materials used: (a) HAP-1; (b) HAP-3; (c) HAP-4; (d) HAP-5; (e) HAP-6; (f) HAP-7. Photograph of HAP-2 was omitted; the surface state of HAP-2 by SEM observation was very similar to that of HAP-1. The bars indicate 0.5 μm.

(binding capacity) on HAP were measured by the following method. Various amounts of protein dissolved in 10 m*M* sodium phosphate buffer solution (pH 6.8; $H_2PO_4^-/HPO_4^{2-}$ molar ratio = 12:7) were applied to the column. The column was then eluted with 10 m*M* pure sodium phosphate buffer solution (pH 6.8) at a flow-rate of 1 ml/min for 30 min. As the 10 m*M* phosphate concentration in the buffer solvent cannot elute any of the adsorbed proteins used in this study, no peak appears when the loaded proteins are all adsorbed on HAP. When the limiting load is exceeded, peaks due to excess and unbound proteins can be detected.

TABLE II

PROTEINS USED

Most data on molecular weight (*M*), frictional ratio (f/f_0) and partial specific volume of the molecule ($\tilde{v}$) were taken from ref. 11. Stokes radius (*r*) was calculated using eqn. 2. p*I* = isoelectric point.

Protein	*Source*	*pI*	*M* (· 10^4)	f/f_0	$\tilde{v}$	*r* (Å)
Serum albumin	Bovine serum	4.7–4.9	6.6	1.288	0.733	34.5
Trypsin inhibitor	Soy bean	4.3–4.6	2.1–2.2	1.2–1.3	0.70–0.74	21.6–24.2
Transferrin	Human serum	5.2	8–9	1.23–1.37	0.73	35.1–40.6
Myoglobin	Horse muscle	7.3	1.78	1.105	0.741	19.2
α-Chymotrypsinogen A	Bovine pancreas	9.5	2.57	1.193	0.721	23.2
Ribonuclease A	Bovine pancreas	9.5–9.6	1.37	1.066	0.707	16.7
Lysozyme	Chicken egg	11.0–11.4	1.43	1.21	0.703	19.2

Surface areas

Total surface areas were measured by the BET method. The accumulation of surface areas based on small pores existing in the HAP were determined by the Cranston–Inkley method[12], assuming a cylindrical pore shape. In the Appendix, the calculation method is briefly explained. They were measured by nitrogen adsorption at 77 K.

Phases and X-ray scattering intensities

Crystalline phases of samples and X-ray scattering intensities of $(10\bar{1}0)$ and (0002) reflections of HAP were obtained on a Rigaku Denki diffractometer with Cu-Kα radiation and a graphite monochromator.

Hydroxyl groups

The intensities of the hydroxyl stretching frequency (3572 cm^{-1}) of powdered HAP samples in CaF_2 discs (5 mg per 500 mg of CaF_2) were measured by the diffuse reflectance method on a Perkin-Elmer Fourier transform (FT)/IR spectrophotometer.

Determination of the surface area available for adsorption

The binding capacities for proteins are related to the surface area necessary for the adsorption of protein molecules on HAP. Assuming the shape of the protein molecules to be a sphere with a Stokes radius, that no interactions occur among them and that there is monolayer adsorption on HAP, the surface area occupied by the maximum amount of globular proteins adsorbed on the HAP surface (S_{capa}) can be estimated from the equation

S_{capa} = (surface area occupied by one protein molecule) × (the maximum number of protein molecules adsorbed on HAP surface).

The surface area occupied by one protein molecule with a Stokes radius r can be calculated as $2\sqrt{3}r^2$, assuming closed-packed adsorption of the protein molecules on the HAP surface. Therefore, we obtain

$$S_{capa} = 2\sqrt{3}r^2 \, (W_{capa} \, N_0/M) \tag{1}$$

where W_{capa} is the maximum amount of protein adsorbed on the HAP surface (binding capacity), N_0 is Avogadro's number and M is the molecular weight of the protein. The Stokes radius is represented by

$$r = (f/f_0) \, (3\tilde{v}M/4N_0)^{1/3} \tag{2}$$

where f/f_0 is the ratio of the frictional coefficient for the flow of a molecule to that of a hydrodynamically equivalent sphere and $\tilde{v}$ is the partial specific volume of the molecule.

On the other hand, we consider two types of protein, namely basic and acidic with relatively basic and acidic isoelectric points, respectively, and we assume that all surfaces appearing on an HAP crystal belong to either type of adsorbing surface. The first type of adsorbing surfase is that on which negatively charged adsorbing sites are

arranged and basic proteins are mainly adsorbed. Such main surfaces are those parallel to the {0001} planes. The second type of adsorbing surface is that on which positively charged adsorbing sites are arranged and acidic proteins are mainly adsorbed. Such main surfaces are those parallel to the $\{10\bar{1}0\}$ planes.

If HAP packing materials have neither pores nor lattice defects and all surfaces are active for adsorption of proteins, we can relate S_{capa} with S_{BET} as follows:

$$S_{capa} = S_{BET}p' \tag{3}$$

where S_{BET} is the total surface area of HAP measured by the BET method and p' represents the proportion of the area of the first or second type of adsorbing surface.

However, there are some inactive parts for adsorption on actual HAP crystals owing to the presence of small pores which the tested protein cannot enter. It is assumed that the pores are present uniformly on the HAP crystal surfaces. It is also assumed that the distribution of the pore size occurring in connection with the first type of adsorbing surface is equal to that occurring in connection with the second type of adsorbing surface. In addition to the inactive area that occurs owing to the presence of pores, another type of inactive area exists in the crystal surface structure, owing to lattice defects such as grain boundaries and some deficiencies of lattice OH^- groups. It is assumed that, on each type of adsorbing surface, the distribution of the lattice defects existing on the inside of the pores is equal to that existing on the outside. With these assumptions, S_{capa} for the HAP material on which both pores and lattice defects are present can be described by

$$S_{capa} = (S_{BET} - S_p)px \tag{4}$$

where S_p is the accumulation of surface areas based on small pores existing in the HAP material which the tested protein cannot enter, and p represents the proportion of the area of the first or second type of adsorbing surface under consideration on which pores are present. With the above-mentioned assumptions, the relationship

$$p' = p \tag{5}$$

is fulfilled. The parameter x represents the proportion of the area of the active part of the first or second type of adsorbing surface under consideration on which lattice defects are present. Hence px represents the proportion of the area of the active part of the $S_{BET} - S_p$ surface area for adsorption of basic proteins or acidic proteins. $(S_{BET} - S_p)\,px$ can be considered to be the effective surface area for adsorption of proteins. In this paper, we assume that the minimum pore diameter in which a protein can enter is $2r$. S_p depends on the molecular size of the tested proteins. The parameters p and x are independent of S_p under the above-mentioned assumptions, and they vary with the method of preparation of HAP. The parameter p means p_1 or p_2 where $p_1 + p_2 = 1$ and the subscripts 1 and 2 are used to denote the first and second type of adsorbing surface, respectively. As the effect of a deficiency of lattice OH^- groups on an adsorbing surface is different between {0001} and $\{10\bar{1}0\}$ planes, x depends on the type of protein used as a probe. Consequently, from eqns. 1 and 4,

$$px = S_{capa}/(S_{BET} - S_p) = 2\sqrt{3}r^2 (W_{capa}N_0/M)/(S_{BET} - S_p) \quad (6)$$

S_{BET}, S_p and W_{capa} are known from experiments and r and M are fixed for each kind of protein. Hence px can be calculated from eqn. 6.

HAP packing materials have a certain constant value of p which depends on the preparation method. If the surface state of HAP changes with the preparation conditions, some variation of px must be recognized, mainly because of a change in x.

RESULTS AND DISCUSSION

Effect of heat treatment on HAP surface state

Fig. 2 plots the relative changes of both $S_{BET} - S_p$ and the binding capacities (W_{capa}) of spherical HAPs on heat treatment for lysozyme and BSA. The decrease in W_{capa} for lysozyme was found to have almost the same tendency as that of $S_{BET} - S_p$. However, the decrease in W_{capa} for BSA was greater than that of $S_{BET} - S_p$ for HAP samples heat treated below 900°C. With HAP-5 (heat treated at 1000°C), W_{capa} for BSA was found to increase considerably, although $S_{BET} - S_p$ still decreased. Therefore, the relative change in W_{capa} on heat treatment of HAP could not be explained only by the decrease in $S_{BET} - S_p$. Table III gives the data on binding capacities and surface states of spherical HAPs heat treated at various temperatures. As can be seen, both px and $S_{BET} - S_p$ for HAP samples heat treated below 900°C, calculated by eqn. 6, decreased with increase in temperature. In contrast, the px value of HAP-5 for BSA increased.

The parameters p and x were separately calculated as follows. The value of p_1x(Lys) of HAP-1 was 0.51 for lysozyme whereas p_2x(BSA) was 0.25 for BSA, where x(Lys) and x(BSA) signify the x for lysozyme and BSA, respectively. Thus the range of p was determined to be $0.51 \leqslant p_1 \leqslant 0.75$ and $0.25 \leqslant p_2 \leqslant 0.49$ from the relationships $x \leqslant 1$ and $p_1 + p_2 = 1$. As HAP-1 is sintered bodies of polycrystals and has some inactive surface for adsorption due to grain boundaries and other lattice defects, it is reasonable to evaluate that the maximum value of x is, in real situations of the order of 0.9 or less. In addition, from the HAP crystal structure, the effect of a deficiency of lattice OH^- groups on the state of the adsorbing surface is considered to be more harmful on

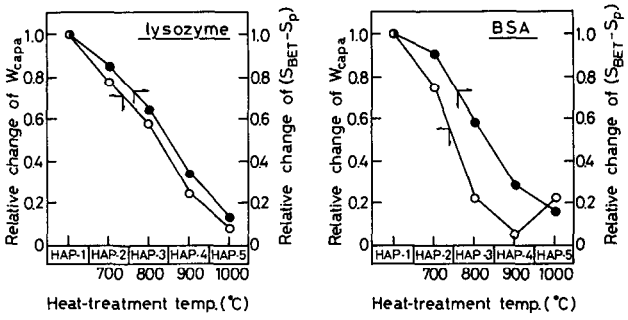

Fig. 2. Relative changes in binding capacities (W_{capa}) and $S_{BET} - S_p$ for lysozyme and bovine serum albumin on heat treatment of HAP-1. The relative change was calculated by dividing W_{capa} or $S_{BET} - S_p$ of HAP heat treated at given temperatures by that of HAP-1.

TABLE III

BINDING CAPACITIES AND PROPERTIES OF SPHERICAL HAP HEAT TREATED AT VARIOUS TEMPERATURES

For details of the measurements of W_{capa} and $S_{BET}-S_p$, see Experimental. S_{capa} and px were calculated using eqns. 1 and 4, respectively.

Protein	*Sample*	W_{capa} *(mg/g)*	S_{capa} *(m^2/g)*	$S_{BET}-S_p$ *(m^2/g)*	$p_1x(Lys)$	p_1	$x(Lys)$
Lysozyme	HAP-1	12.26	6.57	12.9	0.51	0.6	0.85
	HAP-2	9.60	5.14	11.0	0.47	0.6	0.78
	HAP-3	7.11	3.81	8.3	0.46	0.6	0.77
	HAP-4	2.99	1.60	4.3	0.37	0.6	0.62
	HAP-5	1.04	0.56	1.7	0.33	0.5	0.66
Protein	*Sample*	W_{capa} *(mg/g)*	S_{capa} *(m^2/g)*	$S_{BET}-S_p$ *(m^2/g)*	$p_2x(BSA)$	p_2	$x(BSA)$
BSA	HAP-1	5.38	2.01	7.9	0.25	0.4	0.63
	HAP-2	4.02	1.51	7.2	0.21	0.4	0.53
	HAP-3	1.16	0.43	4.6	0.09	0.4	0.23
	HAP-4	0.26	0.10	2.2	0.05	0.4	0.13
	HAP-5	1.19	0.45	1.3	0.35	0.5	0.70

$\{10\bar{1}0\}$ than on $\{0001\}$ planes. Thus, $x(BSA) < x(Lys)$ is realized. Hence the range of p was limited to be $0.56 < p_1 < 0.67$ and $0.33 < p_2 < 0.44$. From these inequalities, p values for HAP-1 were estimated to be 0.6 for p_1 and 0.4 for p_2 with an uncertainty of about ± 0.05.

The X-ray diffraction analysis indicated that the HAP phase of HAP-1–4 did not decompose, as shown in Table I. Further, their intensity ratio, $I_{0002}/I_{10\bar{1}0}$, was found not to change significantly. Hence the value of p was considered to remain almost constant for heat treatments below 900°C.

The value of x of HAP-1–4 for lysozyme and BSA decreased with increasing treatment temperature. The change was particularly large for BSA. For example, only 13% of the adsorbing surface was available for BSA in HAP-4. From the weight loss in thermogravimetric analysis and the decrease in intensity of the hydroxyl stretching frequency (3572 cm^{-1}) in FT-IR analysis, which occurred to heat-treated HAP samples as shown in Table I, the decrease in x can be interpreted by the lattice defects caused by some hydroxyl deficiencies in a crystal. The deficiencies of lattice OH^- groups were extended with increasing heat-treatment temperature. According to the FT-IR analysis of HAP-1–4 after being used for high-performance liquid chromatographic (HPLC) measurements, it was found that the intensities of the hydroxyl stretching frequency increased by about 4–12% compared to that of the new material. These results indicate that, once a loss of lattice OH^- groups has occurred during heat treatment, its complete recovery could not take place although OH^- groups were partly taken into HAP crystals from the phosphate buffer solution.

The p and x values for HAP-5 were similarly determined as follows. As measured by FT-IR spectrophotometry, as many as 55% of the OH^- groups were lost from the crystal surface of HAP-1 during heating at 1000°C. A high deficiency of OH^- groups is

known to cause decomposition of the HAP crystal[10]. In fact, slight decomposition to α-tricalcium phosphate (α-TCP) in HAP-5 was detected by X-ray diffraction analysis. α-TCP is reported to change to HAP again in aqueous solution[13]. In this experiment, the main peak of α-TCP produced in HAP-5, which was weakly detected by X-ray diffraction analysis, had almost disappeared after the material had been used for HPLC. The planes most commonly developed on the crystal exterior in the first stage of crystallization of HAP are those described by the Miller indices $\{10\bar{1}0\}$. Hence p_2 of HAP-5 is considered to become greater than that of HAP-1 because of the generation of new HAP surfaces due to dissolution of α-TCP. From the data on px for HAP-5, the range of p for HAP-5 was determined to be $0.33 \leqslant p_1 \leqslant 0.65$ and $0.35 \leqslant p_2 \leqslant 0.67$ using the procedure used for HAP-1. This range is clearly different from that for HAP-1. Further, from the above experimental analysis, it was considered that p_2 for HAP-5 $> p_2$ for HAP-1 and p_1 for HAP-5 $< p_1$ for HAP-1. Hence the range of p was limited to $0.4 < p_1 < 0.6$ and $0.4 < p_2 < 0.6$. From these inequalities p values for HAP-5 were estimated to be approximately $p_1 = p_2 = 0.5$.

An increase in the x values of HAP-5 was also observed. This may be due to the repairing of the HAP-5 surface when it is used in the phosphate buffer solution. This was supported by the experimental result that the recovery of the intensity of the OH^- frequency was so large compared with other HAP samples that it reached about 30%. This result can also be seen in Table I.

Change of px by protein types

From the above assumption that the same type of proteins adsorb on the same adsorbing surface of HAP, it is expected that the px values would be almost the same among the same type of proteins but would vary with the protein types. The px values of HAP-3 for each protein used were determined by capacity measurements and are given in Table IV. As expected, similar values of px were obtained among the same type of proteins. The values of px were about 0.51 for basic proteins and 0.14 for acidic proteins.

The x values of HAP-3 for basic proteins (about 0.8–0.9) were higher than those for acidic proteins (about 0.4 or less). The reason may be that the repair of the adsorbing surface for basic proteins is better than that for acidic proteins in a phosphate buffer solution, although both adsorbing surfaces are damaged by heat treatment.

$S_{BET} - S_p$ of HAP-3 is plotted against pore diameter and S_{capa} is plotted against protein size in Fig. 3. S_{capa} of HAP-3 for each protein tested lay according to protein type on two curved lines, which were the $(S_{BET} - S_p)px$ expressed as a function of pore diameter. This indicates that S_{capa} of a globular protein of known size and type can be obtained from Fig. 3. Thus, W_{capa} of HAP-3 for the protein can be determined by calculation using eqn. 1, without measurement, substituting S_{capa} obtained from Fig. 3.

Effect of preparation method on surface state

For comparison of the effect of preparation methods on the surface state of HAP, HAP-6 and -7 prepared by wet processes were tested. The values of W_{capa} of these HAP samples for lysozyme and BSA were measured, and px, p and x were then calculated by the above-mentioned method (Table V).

There was a difference in p between HAP-6 and HAP-1. With HAP-6, p_1 for

TABLE IV

BINDING CAPACITIES AND PROPERTIES OF HAP-3 SURFACE FOR GLOBULAR PROTEINS

Protein	*r* (Å)	W_{capa} (mg/g)	S_{capa} (m^2/g)	$S_{BET}-S_p$ (m^2/g)	*px*	*p*	*x*
Transferrin	37.9	1.72	0.60	4.3	0.14	0.4	0.35
Bovine serum albumin	34.5	1.16	0.43	4.6	0.09	0.4	0.23
Trypsin inhibitor	22.9	2.16	1.10	7.1	0.15	0.4	0.38
Myoglobin	19.2	3.23	1.39	8.3	0.17	0.4	0.43
α-Chymotrypsinogen A	23.2	8.19	3.57	7.0	0.51	0.6	0.85
Lysozyme	19.2	7.11	3.81	8.3	0.46	0.6	0.77
Ribonuclease A	16.7	12.3	5.20	9.5	0.55	0.6	0.92

lysozyme (basic protein) was small whereas p_2 for BSA (acidic protein) was so large that it reached 83% of $S_{BET} - S_p$. This was supported by SEM observations. Most surfaces appearing on a hexagonal pillar-shaped HAP-6 crystal (Fig. 1e) were considered to belong to those parallel to the $\{10\bar{1}0\}$ planes.

HAP-7 was considered to be prepared by a wet process different from that for HAP-6. It consisted of very fine pillar-shaped crystals as shown in Fig. 1f. The proportion of the area of the active part of the $S_{BET}-S_p$ surface, *px*, was very small (about 0.2) for both protein types. The calculated *p* ranges were too large to calculate *p* and *x* separately. Hence in this instance some additional information from other experiments is necessary for the determination of reasonable *p* values.

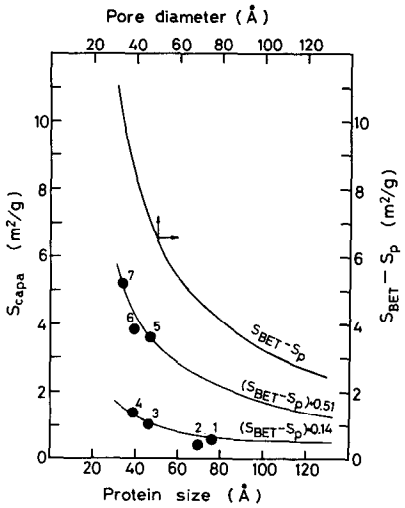

Fig. 3. Relationship between $S_{BET}-S_p$ and pore diameter of HAP-3 and relationship between S_{capa} for tested protein and protein size for HAP-3. Depending on protein type, S_{capa} of HAP-3 for the tested proteins lay on either of the curved lines which show $(S_{BET}-S_p)px$ as a function of pore diameter; *px* is 0.51 for basic proteins and 0.14 for acidic proteins. Proteins: 1 = transferrin; 2 = BSA; 3 = trypsin inhibitor; 4 = myoglobin; 5 = α-chymotrypsinogen A; 6 = lysozyme; 7 = ribonuclease A.

TABLE V

BINDING CAPACITIES AND PROPERTIES OF THE SURFACE OF HAP-6 AND HAP-7

Sample	*Protein*	W_{capa} *(mg/g)*	S_{capa} *(m^2/g)*	$S_{BET}-S_p$ *(m^2/g)*	*px*	*p*	*x*
HAP-6	Lysozyme	1.70	0.91	5.54	0.16	0.17	0.94
	BSA	8.50	3.19	3.85	0.83	0.83	1.00
HAP-7	Lysozyme	8.53	4.57	23.3	0.20	(0.5)[a]	(0.40)[a]
	BSA	7.75	2.90	15.4	0.19	(0.5)[a]	(0.38)[a]

[a] Low reliability. The range of *p* was too large to calculate the exact value of *p* in the case of HAP-7.

Correlation between W_{capa} and S_{BET}

In order to examine whether W_{capa} depends on S_{BET} of HAP, the values of W_{capa} and S_{BET} among the HAP samples were compared. For instance, W_{capa} of HAP-6 for BSA was not very different from that of HAP-7, but S_{BET} of HAP-6 was only about one quarter of that of HAP-7. Further, in spite of the fact that the value of S_{BET} of HAP-1 was smaller than that of HAP-7, W_{capa} of HAP-1 for lysozyme was larger than that of HAP-7. Other similar experimental results were also obtained. Hence no correlation was found between W_{capa} for globular proteins and S_{BET} of HAP.

CONCLUSION

The state of the adsorbing surface of HAP could be established from the effective surface area described as $(S_{BET} - S_p)\,px$. The binding capacities for globular proteins could be related to the effective surface area, not to the BET surface area, as follows:

$$W_{capa} = (M/2\sqrt{3}r^2N_0)\,(S_{BET} - S_p)px \equiv A(S_{BET} - S_p)\,px$$

where $A \equiv M/2\sqrt{3}r^2N_0$ is fixed for each protein.

The proportion of the area of the active part of the $S_{BET} - S_p$ surface area for adsorption, *px*, was similar among the same type of proteins but varied with the protein type, which was expected from the idea that the same adsorbing surface was related to the adsorption of the same type of proteins.

The *px* values obtained in this study contained some inaccuracies. This may be due to the errors accompanying the measurements of S_{BET}, S_p and W_{capa} and the uncertainty in the calculation of S_{capa}. For the determination of S_{capa}, for example, if we take into consideration the repulsive interactions which actually exist among proteins adsorbed on HAP, S_{capa} becomes larger than that calculated by eqn. 1. This results in *x* being calculated to be higher than the value given in this study. Further, S_{capa} becomes different if we calculate the surface area occupied by one protein molecule based on the shape of an ellipsoid. Although the numerical values themselves have some uncertainties such as this, it is still true that *px* is dependent on the preparation methods, the preparation conditions and also the protein types.

APPENDIX

The Cranston–Inkley method[12] is an improved method of deriving pore-size distributions from adsorption isotherms. It can be summarized as follows.

We consider an adsorption step from a relative pressure P_r to a pressure $P_{r+\delta r}$. It is assumed that pores in this range become filled with condensate, whereas in the pores having radii larger than $r+\delta r$ the thickness of the adsorbed layer on their walls increases from t_r to $t_r+\delta t$. Thus, $v_r\delta r$, the volume of nitrogen adsorbed between P_r and $P_{r+\delta r}$, is given by

$$v_r\delta r = \frac{(r - t_r)^2}{r^2} V_r\delta r + \delta t \int_{r+\delta r}^{\infty} \frac{(r - t_r)}{r} \cdot \frac{2V_r}{r} \cdot \mathrm{d}r \qquad \text{(A1)}$$

where $V_r\delta r$ is the total volume of pores having radii between r and $r+\delta r$. The first term on the right-hand side represents the volume of nitrogen due to the effect of capillary condensation and the second term represents the volume of nitrogen due to the effect of multi-layer adsorption.

We then consider a finite adsorption step from pressure P_1 (corresponding to radius r_1) to pressure P_2 (corresponding to r_2). Further, assuming V_r is sensibly constant over the range r_1 to r_2, eqn. A1 becomes

$$v_{12} = \frac{V_{12}}{r_2 - r_1} \int_{r_1}^{r_2} \frac{(r - t_1)^2}{r^2} \cdot \mathrm{d}r + (t_2 - t_1) \int_{r_2}^{\infty} \frac{V_r\,(2r - t_1 - t_2)}{r^2} \cdot \mathrm{d}r \qquad \text{(A2)}$$

where V_{12} is the volume of pores having radii between r_1 and r_2. Rearranging this equation gives

$$V_{12} = R_{12}\left(v_{12} - k_{12} \int_{r_2}^{\infty} \frac{r - t_{12}}{2r^2} \cdot V_r\mathrm{d}r\right) \qquad \text{(A3)}$$

where $R_{12} = (r_2 - r_1)\Big/\int_{r_1}^{r_2}[(r - t_1)^2/r^2]\mathrm{d}r$, $k_{12} = 4\,(t_2 - t_1)$, and $t_{12} = 1/2\,(t_1 + t_2)$. v_{12} can be derived from experimental measurements.

It is convenient to replace the integral term in eqn. A3 by a summation term of all pore increments and to use pore diameter instead of pore radius. Thus, eqn. A3 becomes

$$V_{12} = R_{12}\left(v_{12} - k_{12} \sum_{d_2 + \frac{1}{2}\Delta d}^{d_{max}} \frac{d - 2t_{12}}{d^2} \cdot V_d\Delta d\right) \qquad \text{(A4)}$$

R_{12}, k_{12} and the function $(d-2t)/d^2$ for mean values of t and d have been tabulated for standard pore diameter increments[12]. Thus, S_{12} (surface area in units of m^2/g) can be calculated from eqn. A4 by using the relationship

$$S_{12} = 4aV_{12} \cdot 10^4/d'$$

where a is the ratio of the density of gaseous nitrogen at NTP to that of liquid nitrogen and d' is the mean pore diameter between d_1 and d_2 (Å). The reader is referred to the original paper[12] for the exact details of the calculations.

In our work, the S_p value for each tested protein based on pores existing in the HAP was obtained by accumulating the S_{12} values over a range of pore diameters which is smaller than the size of the tested protein molecule.

REFERENCES

1 T. Kawasaki, *J. Chromatogr.*, 151 (1978) 95.
2 T. Kawasaki, *J. Chromatogr.*, 157 (1978) 7.
3 M. Kukura, L. C. Bell, A. M. Posner and J. P. Quirk, *J. Phys. Chem.*, 76 (1972) 900.
4 A. L. Boskey and A. S. Posner, *J. Phys. Chem.*, 80 (1976) 40.
5 D. M. Roy, L. E. Drafall and R. Roy, in A. M. Alper (Editor), *Refractory Materials*, Vol. 6-V, Academic Press, New York, 1978, pp. 187–206.
6 T. Kawasaki, W. Kobayashi, K. Ikeda, S. Takahashi and H. Monma, *Eur. J. Biochem.*, 157 (1986) 291.
7 Y. Kato, K. Nakamura and T. Hashimoto, *J. Chromatogr.*, 398 (1987) 340.
8 S. Inoue and A. Ono, *U.S. Pat.*, 4 711 769 (1987).
9 N. Tagaya, H. Kuwahara, T. Hashimoto, N. Komatsu, K. Fukamachi and T. Maeshima, *U.S. Pat.*, 4 794 171 (1988).
10 S. Shimabayashi and M. Nakagaki, *Nippon Kagaku Kaishi*, (1978) 326.
11 H. A. Sober (Editor), *Handbook of Biochemistry*, CRC Press, Cleveland, OH, 1973, p. C-10.
12 R. W. Cranston and F. A. Inkley, *Adv. Catal.*, 9 (1957) 143.
13 H. Monma and T. Kanazawa, *Yogyo Kyokai Shi*, 84 (1976) 209.